

Notes

Ferric Phosphite: Dimers of Face-Sharing $\text{Fe}^{\text{III}}\text{O}_6$ Octahedra. Crystal Structure Redetermination, Mössbauer Spectra, Magnetic Susceptibility, and Heat Capacity Data

Jürgen Ensling,¹ Philipp Gütlich,¹ Roswitha Schmidt,² and Rüdiger Kniep²

Institut für Anorganische Chemie und Analytische Chemie, Johannes Gutenberg-Universität, D-55099 Mainz, Germany, and Eduard-Zintl-Institut, Technische Hochschule, D-64289 Darmstadt, Germany

Received September 16, 1993

Phosphophyllite ($\text{Zn}_2\text{Fe}(\text{PO}_4)_2 \cdot 4\text{H}_2\text{O}$) is the main component of the "protective layers" which are formed during "zinc-phosphating" of iron (steel) materials. Further processing of the phosphated metals includes changes of conditions which may cause phase transformations of the primary phosphate phase and which in special cases (paint-baking; $T_{\text{max}} = 180^\circ\text{C}$) may be regarded as "hydrothermal treatment" of the "protective layers".

In the course of our investigations^{3,4} in hydrothermal phase changes of phosphophyllite, we also extended our interest to the reaction of phosphophyllite with phosphorous acid (H_3PO_3) under hydrothermal conditions. We obtained the title compound as plated hexagonal prisms. After our crystal structure determination of $\text{Fe}_2(\text{HPO}_3)_3$ was completed, the work of Sghyor et al.⁵ was published on the same subject. Both crystal structure determinations are of comparable quality and show that $\text{Fe}_2(\text{HPO}_3)_3$ contains Fe_2O_9 units which consist of two face-sharing $\text{Fe}^{\text{III}}\text{O}_6$ octahedra.

This interesting feature of the structure of ferric phosphite directed our attention to the analysis of the magnetic properties of the compound using Mössbauer spectroscopy, susceptibility, and heat capacity measurements. In the following we shall describe and interpret results from these studies.

$\text{Fe}_2(\text{HPO}_3)_3$ was obtained by hydrothermal treatment of phosphophyllite ($\text{Zn}_2\text{Fe}(\text{PO}_4)_2 \cdot 4\text{H}_2\text{O}$) with phosphorous acid. The starting material, phosphophyllite, was prepared as described elsewhere.⁴ A 275-mg sample of phosphophyllite and 5 mL of 1 M H_3PO_3 were placed into a glass tube (degree of filling $\approx 65\%$); the tube was sealed and heated at 180°C (baking oven) for a period of 5 h. The hydrothermally grown crystals of $\text{Fe}_2(\text{HPO}_3)_3$ (up to 0.3 mm in diameter) exhibit a platelike hexagonal-prismatic habit, are translucent, and are white to pale pink.

The crystal structure was solved at room temperature. The compound crystallizes in the hexagonal system, space group $P6_3/m$, with lattice constants of $a = 803.7(5)$ pm and $c = 738.9(5)$ pm where $Z = 2$ ($D_x = 2.83$ g/cm³). Least-squares refinement with 440 observed reflections gave $R = 0.048$. The structure contains $\text{Fe}^{\text{III}}\text{O}_6$ octahedra which share common faces and form Fe_2O_9 units. The intradimer Fe–Fe distance is 298.0(2) pm. The Fe_2O_9 units are interconnected by sharing common apices with HPO_3 tetrahedra, resulting in a three-dimensional arrangement which is shown in Figure 1. The interdimer Fe–Fe distance is 441 pm.

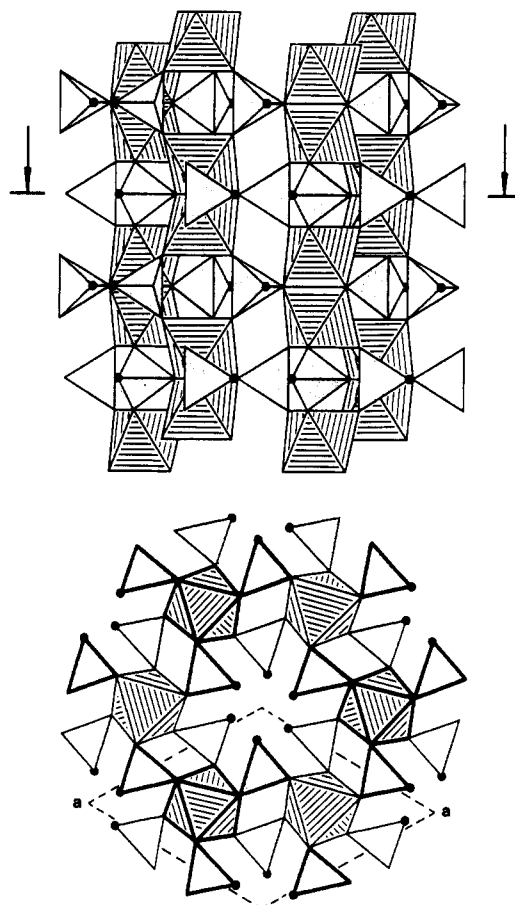


Figure 1. Polyhedral representations (FeO_6 octahedra and HPO_3 tetrahedra) of sections of the crystal structure of $\text{Fe}_2(\text{HPO}_3)_3$: views along $[110]$ (top) and along $[001]$ (bottom). Black dots: H atoms of the HPO_3 groups.

A series of temperature-dependent Mössbauer spectra of $\text{Fe}_2(\text{HPO}_3)_3$ are shown in Figure 2. From 293 K down to approximately 20 K the compound shows a slightly broadened resonance line in the spectra, with an isomer shift typical for octahedral high-spin iron(III) compounds ($\delta = 0.36$ mm s⁻¹ at 293 K, relative to metallic iron). The quadrupole splitting is approximately 0.3 mm s⁻¹ (293 K), indicating a local ferric ion coordination of nearly cubic symmetry. In order to study the onset of magnetic ordering, detailed low-temperature measurements were made. The completely hyperfine-split Mössbauer spectrum develops within 1 K (see Figure 2), although with very broad lines resulting probably from relaxation effects due to fluctuation rates of the internal field comparable to the Mössbauer frequency window ($\approx 10^7$ s⁻¹). A distribution of the hyperfine field caused by slightly different surroundings of the ferric ions in the crystals can be excluded on the basis of the well-defined structure of the compound. The superposition of paramagnetic (doublet) and magnetically ordered (sextet) portions of the spectra in this transition region suggests that not all zones in the crystals of the powder exhibit 3D ordering simultaneously; there are domains which still behave paramagnetically and domains which are already ordered. In order to obtain the Mössbauer parameters in this transition region, the spectra were analyzed by utilizing a computer program (NORMOS⁶) which was developed to fit spectra with a distribution of the hyperfine field. The line broadening persists down to 17 K; below that temperature the spectra could be satisfactorily analyzed by assuming a static

(1) Johannes Gutenberg-Universität.
 (2) Technische Hochschule Darmstadt.
 (3) Schmidt, R.; Eisenmann, B.; Kniep, R.; Ensling, J.; Gütlich, P.; Seidel, R. *Z. Naturforsch.* **1990**, *45B*, 1255.
 (4) Schmidt, R.; Kniep, R. *Z. Naturforsch.* **1992**, *47B*, 445.
 (5) Sghyor, P. M.; Durand, J.; Cot, L.; Rafiq, M. *Acta Crystallogr.* **1991**, *C47*, 2515.

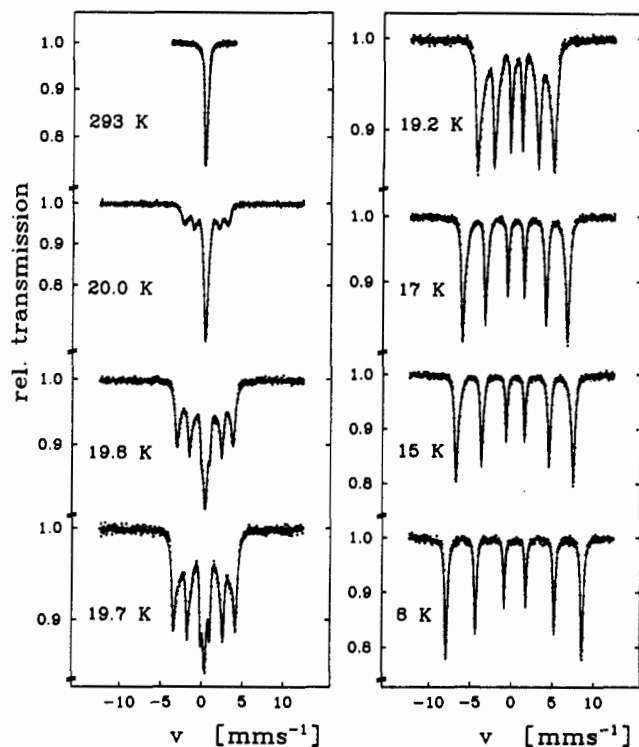


Figure 2. Mössbauer spectra of $\text{Fe}_2(\text{HPO}_3)_3$ recorded at different temperatures.

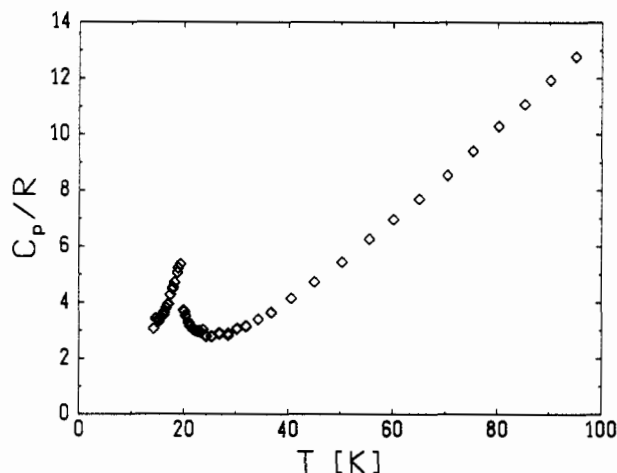


Figure 3. Molar specific heat of $\text{Fe}_2(\text{HPO}_3)_3$ as a function of temperature.

hyperfine field (fit program MOSFUN⁷). In a plot of the hyperfine field versus temperature the Néel temperature of the paramagnetic-to-antiferromagnetic transition, can be assigned as $T_N = 20.02 \pm 0.05$ K. The hyperfine field reaches a saturation value at $T = 0$ K of ≈ 540 kG, a value which is expected for high-spin iron(III) where the Fermi contact term represents the main contribution to H_{eff} .

The specific heat of $\text{Fe}_2(\text{HPO}_3)_3$ is presented in Figure 3. The observation of a λ -anomaly indicates a long-range ordering, the transition temperature of which can be identified from the maximum of the peak in the heat capacity curve⁸ and is found to be 19.7 K.

Variable-temperature magnetic susceptibility data were collected for a 76-mg sample of $\text{Fe}_2(\text{HPO}_3)_3$ with a vibrating-sample magnetometer (Foner magnetometer, Princeton Applied Research). The 3D ordering observed in the temperature-dependent Mössbauer spectra is confirmed by the magnetic susceptibility

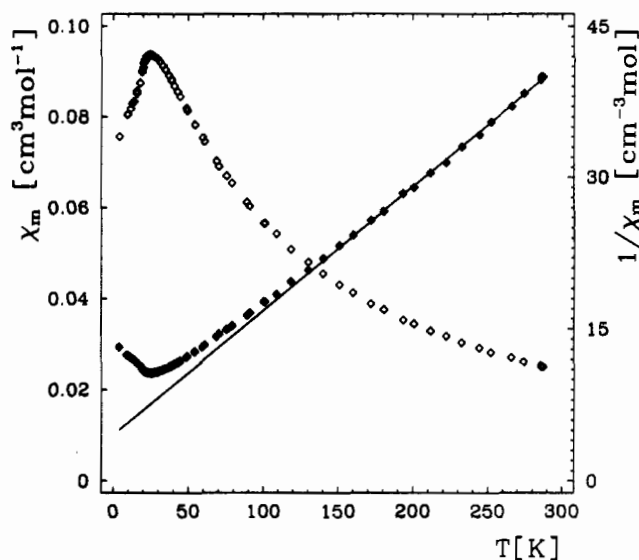


Figure 4. Plots of the magnetic susceptibility data of $\text{Fe}_2(\text{HPO}_3)_3$ (applied field 1 T): (\diamond) χ vs. T ; (\blacklozenge) χ^{-1} vs. T . The solid line through the experimental curve (\blacklozenge) is generated from a least-squares fit of the data to the Curie-Weiss equation.

data. The $\chi(T)$ curve (see Figure 4) exhibits a rather sharp maximum at about 23 K, decreasing to approximately two-thirds of χ_{max} at 0 K. This behavior is typical for a long-range antiferromagnetic ordering in a powder sample.⁸ The transition temperature T_N lies somewhat on the low-temperature side of the maximum where $\chi(T)$ has its maximum positive slope. The estimated value turns out to be 19.7 K, in good agreement with the results of Mössbauer and heat capacity studies.

The attempt to analyze the susceptibility data on the basis of the isotropic Heisenberg-Dirac-Van Vleck (HDVV) dimer model for an $S_1 = S_2 = 5/2$ system (from 35K—well above the transition region—up to room temperature), including the correction for interdimer exchange (molecular field approximation),⁹ resulted in a weak antiferromagnetic exchange coupling ($J \approx -2$ cm⁻¹) within the dimer units and an interdimer coupling of the same order of magnitude, showing that the applied model is not appropriate for this system. The three-dimensional ordering at 20 K obscures the characteristic temperature behavior of the intradimer coupling in the dimeric high-spin iron(III) entities. Pretransitional effects cause a pronounced deviation of the experimental susceptibility from the calculated susceptibility for an isolated dimer as T_N is reached. The Curie-Weiss equation $\chi = C/(T - \Theta)$, where $C = Ng^2\beta^2S(S+1)/3k$, was fit to the experimental magnetic susceptibility in a temperature range well above T_N (150–300 K) with use of a least-squares fitting program (MINUIT¹⁰), yielding the best-fit parameters $C = 4.07$ cm³ mol⁻¹ K and $\Theta = -36$ K (with $g = 2.002$) by minimizing the function $\sum[(\chi_i(\text{obsd}) - \chi_i(\text{calcd}))^2/\chi_i(\text{obsd})^2]$. The smaller value of the Curie constant as compared to the theoretical spin-only value (4.38 cm³ mol⁻¹ K) can be ascribed to a weak antiferromagnetic exchange coupling between the iron atoms in the dimeric units of the compound. Using the connection between the Curie constant Θ and the exchange coupling constant J of the HDVV dimer model in the high-temperature limit, being $\Theta = 35J/k$ ($J \gg kT$, or $T \gg T_N$), a value for J of about -4 cm⁻¹ can be estimated.

The weak antiferromagnetic exchange coupling results from the nearly 90° superexchange interaction Fe(III)-O-Fe(III) via the three O atoms of the phosphite ligands which form the common face of two octahedra. In such a geometrical arrangement, a ferromagnetic interaction should prevail.¹¹ However, the presence

(6) Brand, R. A. Technical Report; KfK, Jülich, 1989.

(7) Müller, E. W. *Mössbauer Eff. Ref. Data J.* 1981, 4, 89.

(8) Carlin, R. L. *Magnetochemistry*; Springer-Verlag: Berlin, Heidelberg, New York, Tokyo, 1986.

(9) Hatfield, W. E. In *Theory and Application of Molecular Paramagnetism*; Boudreaux, E. A., Mulay, L. N., Eds.; John Wiley & Sons: New York, 1976; Chapter 7.

(10) CERN Program Library, Entry D506, Geneva, 1989.

of direct interaction between the metal orbitals in the dimeric units (rather short Fe-Fe distance of 298 pm) may push the system near the antiferromagnetic to ferromagnetic crossover. An enhanced electron density on the bridging O atom due to the electron-donating property of phosphorus in the phosphite ligand—compared to a pure oxo bridge—can also promote an antiferromagnetic exchange interaction.

The observed magnitude of the antiferromagnetic exchange coupling in $\text{Fe}_2(\text{HPO}_3)_3$ fits very well into the general trend found for various mono- and dibridged Fe(III) complexes (cf. refs 12

and 13 and references therein). Monooxo-bridged iron(III) dimers with a bridging angle between 180 and 140° mediates the largest antiferromagnetic exchange coupling ($J = -80$ to -150 cm^{-1}), whereas dihydroxy-bridged dimers with bridging angles around 103° exhibit a smaller extent of exchange, $\approx -10 \text{ cm}^{-1}$. Our value of $\approx -4 \text{ cm}^{-1}$ for $\text{Fe}_2(\text{HPO}_3)_3$ with 90.3° angles falls on this line.

The pathway for the observed long-range ordering at about 20 K clearly indicates that the phosphorus atoms of the phosphite ligands connect Fe_2O_9 units throughout the crystal. This three-dimensional interaction sets in well above the transition point, as shown by the marked deviation from the Curie-Weiss behavior.

Acknowledgment. We wish to thank Prof. Dr. W. E. Hatfield for valuable discussions.

-
- (11) Hay, P. J.; Thibault, J. C.; Hoffmann, R. *J. Am. Chem. Soc.* **1975**, *97*, 4884.
(12) Borer, L.; Thalken, L.; Ceccarelli, Ch.; Glick, M.; Zhang, J. H.; Reiff, W. M. *Inorg. Chem.* **1983**, *22*, 1719.
(13) Adler, J.; Enslin, J.; Gütlich, P.; Bominaar, E. L.; Guillin, J.; Trautwein, A. X. *Hyperfine Interact.* **1988**, *42*, 869.